JOURNAL OF COLLOID AND INTERFACE SCIENCE **208,** 23–33 (1998)
ARTICLE NO. CS985717

Effects of Substratum Topography on Bacterial Adhesion

Teresa R. Scheuerman,[1] Anne K. Camper,[2,3] and Martin A. Hamilton[2]

Center for Biofilm Engineering, Montana State University, 366 EPS Building, Bozeman, Montana 59717-3980

Received February 5, 1998; accepted June 19, 1998

The effect of substratum topography on bacterial surface colonization was studied using a chemically homogeneous silicon coupon. "Grooves" 10 μm deep and 10, 20, 30, and 40 μm wide were etched on the coupon perpendicular to the direction of flow. Flow (Re = 5.5) of a bacterial suspension (10^8 cells/ml) was directed through a parallel plate flow chamber inverted on a confocal microscope. Images were collected in real time to obtain rate and endpoint colonization data for each of three strains of bacteria: *Pseudomonas aeruginosa* **and motile and nonmotile** *Pseudomonas fluorescens.* **A higher velocity experiment (Re = 16.6) and an abiotic control using hydrophilic, negatively charged microspheres were also performed. Using a colloidal deposition expression, the initial rates of attachment were compared.** *P. aeruginosa* **attached at a higher rate than** *P. fluorescens* **mot+ which attached at a higher rate than** *P. fluorescens* **mot−. For all bacteria the rate was independent of groove size and was greatest on the downstream edges of the grooves. Only the motile organisms were found in the bottoms of the grooves. A higher fluid velocity resulted in an increase in the initial rate of attachment. In contrast, there was no adhesion of the beads. Attachment of the bacteria appears to be predominated by transport from the bulk phase to the substratum.** © 1998 Academic Press

Key Words: **bacterial adhesion; transport; topography.**

INTRODUCTION

Existing literature is confusing and contradictory about the mechanism of bacterial adhesion to hard surfaces in flowing systems. The issue is complicated by the common use of static experimental systems, which eliminate the important effects of hydrodynamics and transport to the substratum, and by the often-used assumption that bacterial cells can be modeled as inert colloidal particles. Whenever a biofilm is formed, the bacteria must be transported to the surface and, once there, interact with the surface so that they can remain and multiply. It has been unclear whether transport is controlling or whether the physicochemical forces are predominant in initial attachment in flowing systems.

There exist two theories regarding the attachment of cells to a substratum, DLVO and thermodynamics. Both rely on descriptions of physicochemical forces. The DLVO theory proposes that adhesion is mediated by attractive Lifshitz–Van der Waals forces as well as attractive or repulsive electrostatic forces. The DLVO theory uses the laws of colloid chemistry and is based upon the "macroscopic" cell surface properties with no regard to cell or substratum surface heterogeneity—chemical or structural. Sjollema and Busscher (31) state that DLVO is not sufficient for explaining deposition phenomena because negatively charged particles have deposited on negatively charged substratum, overcoming the electrostatic repulsion. The thermodynamic theory is based upon the free energy of adhesion by deriving the surface free energies of the cell and substratum surfaces. It has been stated that cell surface appendages or excretion of adhesives assist or impede adhesion in excess of strictly thermodynamic considerations (5). Both theories assume that the transport of the cells to the substratum is not limiting, and that the surface of the cells and the substratum are chemically homogeneous.

Related to the DLVO and thermodynamic theories are the measurable phenomena of surface charge and electrostatic interactions. Electrostatic interactions have been implicated in affecting particle deposition (3). The zeta potential is one way of expressing the charge interaction between bacteria or particles and a substratum. However, it has been shown that there is a possibility of several zeta potentials in the same organism (12). It is also well known that bacteria change their surface composition in response to the environment (11). Cell surface hydrophobicity has also been used to try to define attachment phenomena, but its relative importance is likely low, as (i) there is no clear trend in cell attachment based upon hydrophobicity measurements (4, 27, 36) and (ii) the cell surface hydrophobicity is not necessarily constant for an organism (1, 37). The changeable nature of the charge and hydrophobicity of bacterial surfaces indicates that the use of a theory that strictly defines bacteria as colloids is inappropriate.

One significant manner in which bacteria differ from colloids is the presence of cell structures. It has been theorized that cell appendages may complicate the physicochemical picture of attachment by bridging the distance between the cell and surface because of their small radii or more hydrophobic character than the remainder of the cell (22, 34). However,

[1] Current address: 721 Eastview Ct., Jackson, MO 63755.

[2] Center for Biofilm Engineering, 366 EPS Building, P.O. Box 173980, MSU—Bozeman, Bozeman, MT 59717-3980.

[3] To whom correspondence should be addressed. Fax: (406) 994-6098. E-mail: anne_c@erc.montana.edu.

0021-9797/98 $25.00
Copyright © 1998 by Academic Press
All rights of reproduction in any form reserved.

Piette and Idziak (28) demonstrated that the flagellum is no different from the cell surface in hydrophobicity or surface charge, but the small radius makes it more prone to adhesion than the cell body.

Before the bacteria can interact with the substratum, they must be transported there. The ability of a bacterium suspended in fluid to cross the boundary and diffusion layers and reach the surface is influenced by sedimentation, attractive interactive forces, and a velocity component toward the surface provided by collisions between flowing particles (38). Diffusion is a critical component of cell–surface interaction and can be influenced by cell motility which can act to increase the effective diffusivity of the cells to the surface by up to four orders of magnitude (24, 25). Piette and Idziak (28) have shown that *Pseudomonas fluorescens* flagellated cells attached in greater numbers than deflagellated cells. Because even nonflagellated cells attach, this effect has been attributed entirely to the added ability of motile organisms to reach the surface. The importance of motility in bacterial transport to the surface has also been reported by Camper *et al.* (7).

A factor contributing to transport and potentially to physicochemical effects on attachment is the influence of surface topographical features. It has been hypothesized that bacteria preferentially stick to rougher surfaces for three reasons: (i) a higher surface area available for attachment, (ii) protection from shear forces, and (iii) chemical changes that cause preferential physicochemical interactions. For example, work with bacterial suspensions has shown that a rough surface (matt steel) had 1.44 times more microorganisms attached than a smooth surface (electropolished steel) (27). Adhesion rate constants of *Pseudomonas aeruginosa* to electropolished 316-L stainless-steel plates were about 100 times lower than those to 120-grit surfaces (39). Other work with stainless steel has shown that bacteria were associated with the grain boundaries (16). However, the grain boundaries exhibit not only a change in topography but also a change in chemistry (18). Cells tend to be associated with the chemically heterogeneous weld structures in stainless steel, but the issue is complicated by the presence of stagnant water at the weld crown and roots, particularly where undercut, suck-back, or excessive reinforcement exists (40). It has been hypothesized that cells deposit in milling crevices because they are protected from shear arising from flow (14). A wide range of shear stresses was tested and it was noticed that the cells transported to the surface attached reversibly and were washed off again at rates increasing with the surface shear stress. There was a critical surface shear stress of $6-8$ N/m^2 above which the extent of attachment dropped off sharply (14).

The goals of this investigation were (i) to discover how bacterial adsorption is affected by defined topographical features on a surface for which the surface chemistry is held essentially constant; (ii) to determine the relative importance of bulk water fluid dynamics and bacterial motility on bacterial attachment; and (iii) to assess the ability of strict colloid theory to explain bacterial attachment to surfaces. The experiments used two motile bacterial strains, one nonmotile strain, and an inert colloid. Colonization of an etched silicon coupon in a flow cell was observed through a window in the flow cell. Quantitative image analysis was used to calculate adsorption patterns and rates, and the measures were submitted to statistical analysis.

MATERIALS AND METHODS

Coupon

The effect of substratum topography on bacterial surface colonization was studied using a chemically homogeneous single crystal 1, 1, 1 silicon coupon. This allowed us to create a surface where topography could be engineered independently of surface chemistry. Because the silicon is reflective, it also was amenable to nondestructive time-series microscopic analysis with reflected light. In addition to these features, this material was chosen because contamination of silicon wafers used in the semiconductor industry by particles, including bacteria, is of considerable economic interest. A microscale hydrodynamic model (10, 13) was used to calculate the influence of alternative topographic features on local hydrodynamics. Based on model results, rectangular grooves 10 μm deep and 10, 20, 30, and 40 μm wide perpendicular to the direction of flow were selected. Figure 1 illustrates the modeling results for a 10- and 40-μm-wide groove. Two sets of the four grooves were used; one set increased in size from 10 to 40 μm wide (first half) and the other set decreased from 40 to 10 μm (second half). This pattern has the two widest grooves in the center of the coupon and reduces the effect of any linearity in adhesion across the coupon. Groove size and morphology were verified on a fractured coupon by scanning electron microscopy. The flat surface of the coupon was smooth at the submicrometer level. Grooves were 10 μm deep, and widths were within 20% of the predicted value. The cross-sectional shape of the grooves was more u-shaped than rectangular, but the upper edges were distinct.

Flow Cell and Reactor Configuration

The same parallel plate flow cell, flow conditions, chemostat media (except for glucose which was 0.4 g/L), and chemostat cell growth rate (0.2/h) used in this work were used in a previous study with stainless-steel coupons (6) (Fig. 2). To eliminate settling effects on cell transport, the flow cell was mounted on an inverted confocal laser scanning microscope. Flow conditions were maintained at a Reynold's number of 5.5 (average velocity = 2.78 cm/s, average shear stress = 0.83 N/m^2) for all but one experiment, where a Reynold's number of 16.6 (average velocity = 8.33 cm/s, average shear stress = 2.5 N/m^2) was used. The transport phenomena in a parallel plate flow chamber have previously been described (38).

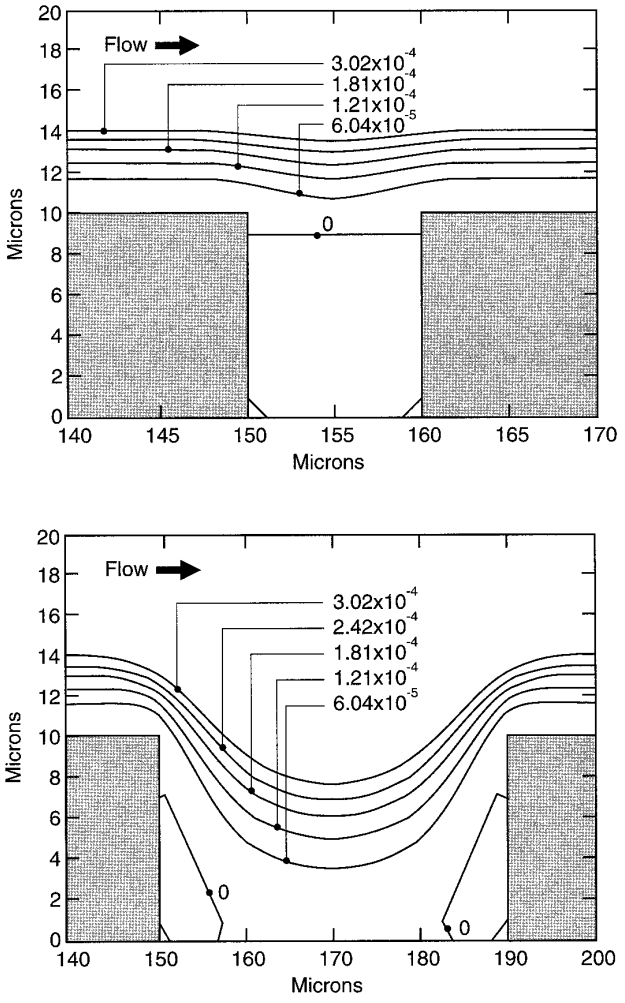

FIG. 1. Simulated stream functions (m^2/s) generated by the microscale hydrodynamic model in the vicinity of 10- and 40-μm-wide grooves at a Reynold's number of 5.5. At steady state, stream functions can be interpreted as streamlines and therefore represent curves actually traced out by particles of fluid.

Cleaning/Disinfection Procedure

As received, the coupons were covered with a protective layer of photoresist. To remove the photoresist, each coupon was first immersed in acetone and then into "pyranha" which is composed of 70% sulfuric acid and 30% hydrogen peroxide. The pyranha was decanted and the coupon was rinsed several times with fresh double-glass-distilled water.

The efficacy of the cleaning procedure was confirmed on selected coupons using a Physical Electronics Laboratories PHI-5600 ESCA spectrometer. A monochromatic Al$K\alpha$ source was operated at 350 W (15 kV, 23.3 mA). The samples were analyzed at a 45° take-off angle which equates to a sampling depth of approximately 60 Å. Chemical homogeneity was confirmed by examination of the bottom of a 40-μm groove and comparison with the analysis of the top plane of the coupon.

System disinfection was accomplished by autoclaving (121°C, P = 23 psi) except for the coupon and the reactor. The reactor was sterilized with methanol (99.9$^+$ HPLC grade, Aldrich) immediately prior to coupon insertion.

Inoculum Preparation

Three strains of aerobic, rod-shaped, gram-negative bacteria were used in the experimentation: *P. aeruginosa* (ERC1 environmental isolate in the culture collection at the Center for Biofilm Engineering, Montana State University, Bozeman, MT) *P. fluorescens* (CC-8404606-E from Darren Korber, University of Saskatoon, Saskatoon, Saskatchewan, Canada) mot+, and *P. fluorescens* mot− (nonmotile transposon mutant of the mot+ strain). Fluorescent beads, spherical and 1 μm in diameter (yellow-green carboxylate-modified, hydrophillic, surface charge density of 6.25 μC/cm^2, actual diameter of 0.997 μm, Molecular Probes), were used instead of bacterial cells to document the location of attachment with respect to hydrodynamics. *P. aeruginosa* is reported to be hydrophilic (15) and possesses an overall net negative charge; therefore, hydrophilic, negatively charged beads were chosen.

Experimental Procedure

Duplicate experiments were conducted with each of the three organisms at a Reynold's number of 5.5; one experiment with *P. aeruginosa* was conducted at a Reynold's number of 16.6. For all experiments, cell concentrations entering the flow cells were measured microscopically after filtering and staining the cells with 0.1% acridine orange in 4% formalin and using an Olympus BH-2 epifluorescence microscope (BP 490 filter, 490 nm, magnification 1000×) and standardized to 10^8/ml. The fluid flowing across the coupon surface consisted of 50% spent chemostat effluent with cells and 50% buffer to minimize cell growth.

To document the potential deposition of any conditioning

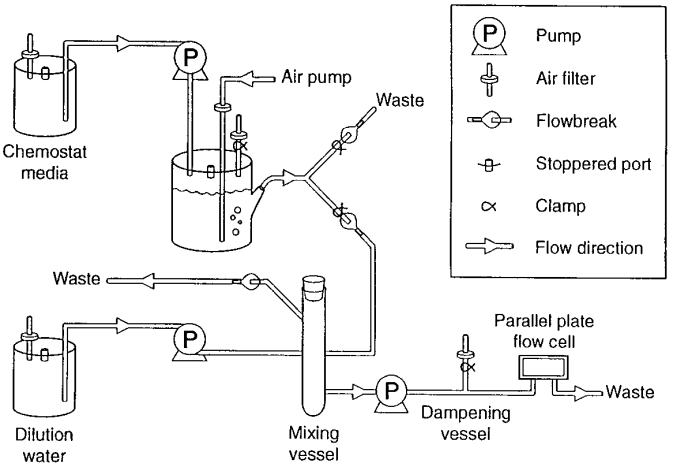

FIG. 2. Schematic of the reactor system.

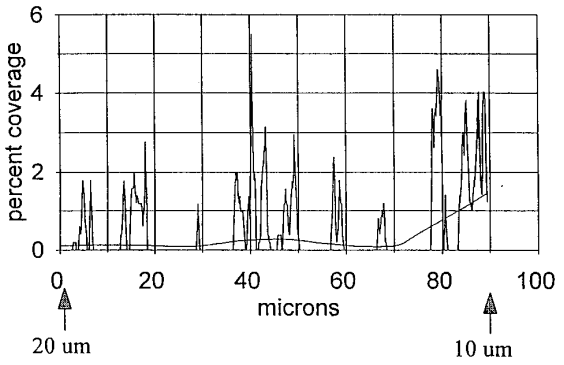

FIG. 3. Sample plot of raw data from the image analysis software (MARK) from an image with the associated LOWESS regression line (downstream of groove 1, *P. fluorescens* mot+ (Experiment H)).

film from the chemostat effluent on the coupons, 0.4-μm pore size filtered *P. aeruginosa* chemostat effluent was allowed to flow over the coupon for 1 h. The coupon was then immediately placed in a filtered reagent-grade nitrogen (99.999%) stream. The coupon was then examined using ESCA as described above.

During the attachment studies, images of the coupon surface were collected in real time under flowing conditions and analyzed. Images were collected approximately every 20–30 min (3 h for nonmotile organisms) with an inverted Biorad confocal scanning laser microscope (MRC 600) using a 50× ULWD objective at a zoom of 2.0. With the two motile organisms, images were collected until cell division was noted (<12 h). The nonmotile bacteria studies were extended for longer times (up to 46 h) but the data used in the analysis were only from the first 12 h. The images were taken in the same horizontal line, parallel to the direction of flow. The first image was collected just upstream of a groove. The second one was collected centered over the groove. The third one was collected between two grooves, and so on. At the next time period, the whole process was repeated. The edge of a groove was always included in each image.

The images clearly showed cells on the coupon surface, but not cells on the bottoms of the grooves. In order to see cells on the bottom of the grooves, it was necessary to perform destructive endpoint staining at the conclusion of the observation period. A recycle loop was created without introducing an air–water interface and 0.1 mL of acridine orange (0.1% acridine orange in 4% formalin) was added to the flow cell. After half an hour the stain was flushed from the flow cell and fluorescent images were taken at the bottom of the grooves and along the top surface of the coupon.

Image Analysis

Advanced image analysis software (MARK, developed in-house) was used to calculate the percentage of a surface area covered by bacteria at fixed distances from the grooves. Because the pixel columns in an image were not always aligned in parallel with the edges of the grooves, some images were rotated using MARK. After rotation, each pixel column was perpendicular to the flow and all pixels in a column were equidistant from the edge of the nearest groove. Using MARK, it was possible to categorize each pixel in a column as either unoccupied substratum or covered by a cell, and to record the percentage of pixels in a column that were covered by cells. An example plot of coverage percentages for all pixel columns between two grooves is shown in Fig. 3. The noise in the percentages occurs because of the narrow width of a pixel column (pixel = 0.165 μm) relative to cell size. By averaging over more than one pixel column, the effect of the noise was greatly reduced. Averaging was done in two steps. First, the raw pixel column percentages were smoothed using a locally weighted scatter plot smoother (LOWESS), where the window width of the smoother was set at $f = 0.4$ in the Minitab computer program (21). An example of the smoothed coverage percentages is shown in Fig. 4. Second, the data were further aggregated by taking an average of the smoothed coverage percentages over 2-μm-wide intervals centered at each of three positions of interest, called *upstream* (6 μm upstream of a groove), *downstream* (6 μm downstream of a groove), or *control* (45 μm from a groove). The averaging was done for each time period and each groove. The three position intervals between grooves 1 and 2 are shown as short, thick lines (at 25% coverage) in Fig. 4.

Data Interpretation

The average surface coverage percentage, calculated as just described, will henceforth be called *coverage.* Statistical analysis was conducted to assess the effects of the following four factors on coverage: time, groove width, position, and half. The factor *half* pertains to whether the location was in the first (upstream) half of the coupon or the second (downstream) half of the coupon.

Analysis of covariance. Because the microscope was moved across the silicon coupon sequentially, each microscope

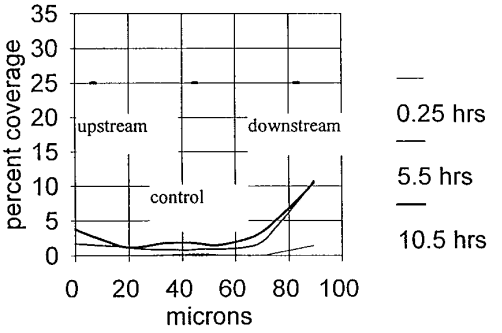

FIG. 4. Sample plot LOWESS lines from a time series showing the values for the positions of the cells on the coupons (downstream of groove 1, *P. fluorescens* mot+ (Experiment H)).

image was captured at a different time. It was necessary, therefore, to adjust the surface coverage percentage for the effect of time, before assessing the effects of groove width, position, and half. Analysis of covariance, with $\log_{10}$-transformed time as the covariate and $\log_{10}$-transformed coverage as the response, was used to accomplish the adjustment (26). To test the null hypothesis that a factor (position, groove size, or half) had no effect on the mean $\log_{10}$ (coverage), a conventional analysis of variance F test was used (26). The analysis of variance showed that interactions among the factors were not statistically important. Statistical diagnostic plots showed that the $\log_{10}$-transformed coverage conformed to the assumptions of homogeneous variance, normality, and linearity required for validity of the analysis of covariance estimates and tests (29).

When the experiment was duplicated, a variance component for between-experiment variation was added to the model. The estimated variance components allowed a comparison of within-experiment variance to the between-experiment variance.

Nonlinear regression analysis. Let $N(t)$ denote the number of cells adsorbed to the substratum in a specified area at time t (h). Meinders *et al.* (20) propose the following equation as a representation of the kinetics of cell adsorption,

$$N(t) = \frac{J}{B}(1 - e^{-Bt}), \qquad [1]$$

where the quantities J, called the *initial coverage rate,* and B are unknown coefficients that could be estimated from experimental data collected at times before cells on the surface began to divide. The constant J in [1] is the slope of $N(t)$ at time zero; that is, $N'(0) = J$. This expression [1] specifies that $N(t)$ reaches a plateau at J/B when t is large.

The analysis of covariance and [1] are very similar expressions for describing how coverage changes as a function of time when $t \leq 12$ h. The analysis of covariance provided a better framework for assessing potential interactions among the factors. It was of primary interest, however, to analyze the initial coverage rate, J, of [1]. Therefore, J and B of expression [1] were estimated for each relevant subset of the data, where coverage was used in place of $N(t)$. The subsets were chosen to represent levels of the factors; e.g., one subset was for the downstream level of the position factor. It was appropriate to consider each level of a factor, aggregated over the other factors, because the analysis of covariance indicated that there were no important interactions among the factors. For most subsets of data, the coefficients B (h^{-1}) and J (coverage per hour) of [1] were estimated using an iterative, nonlinear least-squares routine in the S-plus computer program (19). The program also provided a standard error for each estimate; the standard error calculation was based on a local linear approximation of the nonlinear model (26).

Expression [1] implies that, in the absence of cell division, there is a maximum achievable coverage value (plateau) at J/B. The plateau was estimated for each combination, species $\times$ strain $\times$ Reynold's number. When there were duplicate experiments, the plateau was estimated by dividing the average J by the average B.

For a few subsets of the data, the coverage percentages were linear in time, never approaching the plateau. For those subsets, the nonlinear regression routine was unreliable. Therefore, a conventional least-squares regression line was fit to the data, and the slope of the line was used as an estimate of J.

When comparing values of J estimated from two separate subsets of the data, the ratio of J values was presented, and statistical significance was determined by a two-sample t test (26) of the null hypothesis that the true ratio of J values equals 1.

RESULTS

Bacterial Attachment Experiments

Pseudomonas aeruginosa. Based on endpoint visual inspection of images taken of stained cells (Fig. 5) it was noted that the density of cells in the bottoms of the grooves was similar to the density in the control position on the coupon surface. Using initial coverage rates (J values) averaged for all groove widths and all experiments, it was found that the J values were largest for the downstream edge, followed by the upstream edge, and were lowest for the control position (Table 1). A similar relationship held for the average plateau values; the plateau for the downstream position was higher than the upstream position which was higher than the control position (Table 2). At the lower Reynold's number of 5.5 the J value for the downstream position was also statistically different from that of the control ($P = 0.006$ and 0.001). Although the J value was larger for the upstream edge, it was not statistically different from the control ($P = 0.056$). There appears to be significant preferential attachment to the edges of the grooves, especially downstream.

It was also of interest to note (i) if there was a difference in the initial coverage rates and plateau values for two halves of the coupon or (ii) if groove width influenced these values. For this organism, plateau values for grooves in the first half of the coupon were significantly larger than for grooves in the second half ($P < 0.001$ for the duplicate experiments at Re = 5.5 and the experiment at Re = 16.6). In the case of groove width, analysis of covariance showed that this effect was statistically significant. However, no systematic contribution of groove width to coverage could be found when coverage was plotted vs actual groove width. Therefore, it is likely that this value is the result of noise and inherent variability within the experiments and not the result of an actual importance of groove width on attachment.

Increased flow rate had an effect on the initial coverage rate. At all three positions, the observed J for Re = 16.6 was

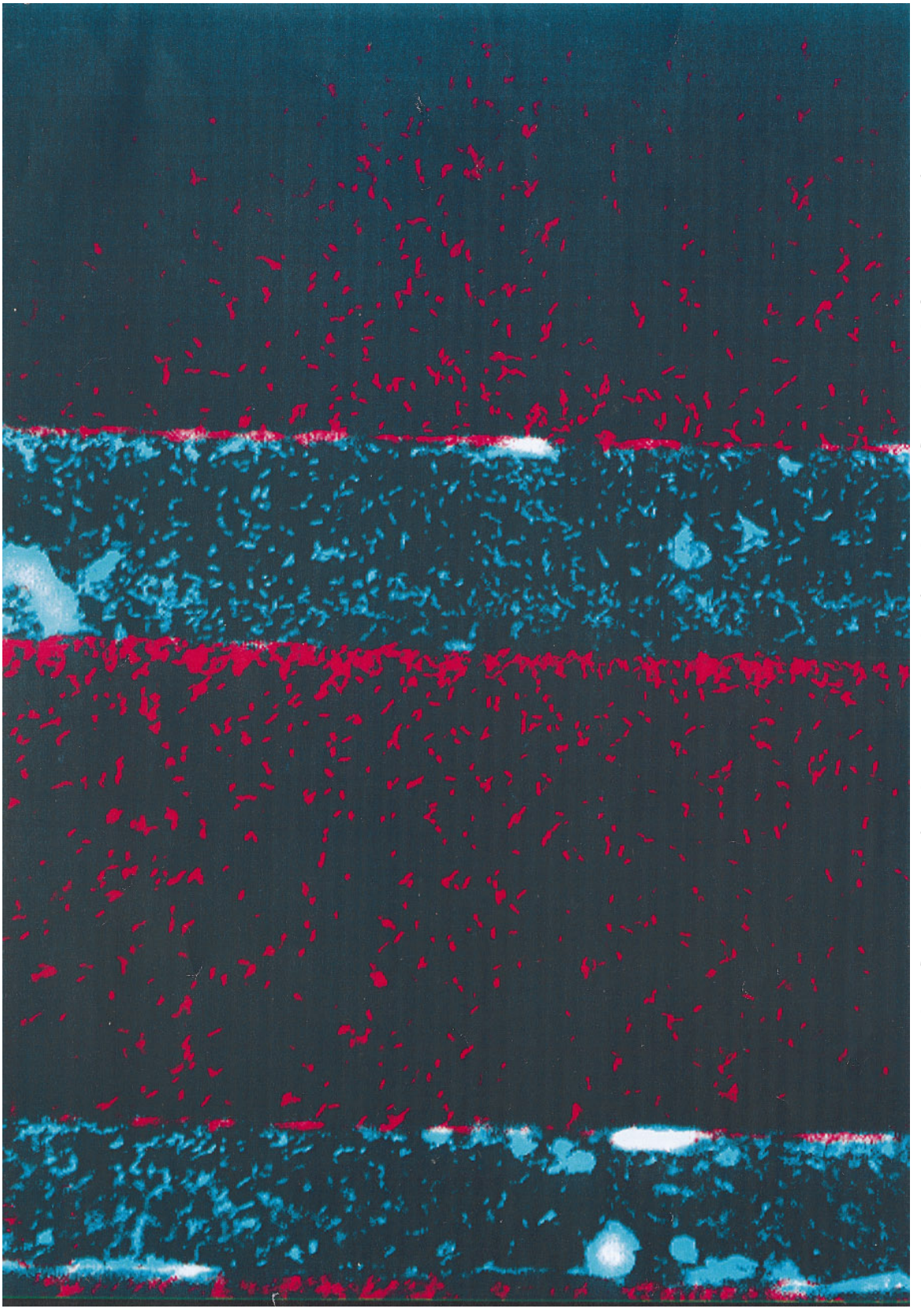

FIG. 5. Representative endpoint fluorescent image of *Pseudomonas aeruginosa* taken after 5.5 h exposure to flow conditions. The figure is a merge of two images; the blue cells are in the bottoms of the grooves and the red cells are on the top plane of the coupon. The groove on the right is 40 μm and the groove on the left is 30 μm. Flow is from right to left.

TABLE 1
Least-Squares Estimates for J (Coverage per Hour) and B (h^{-1}) of Eq. [1] by Position for Each Experiment, with the Standard Error (SE) of Each Estimate

		Regression estimates			
Expt No.	Position	J	SE of J	B	SE of B
		Pseudomonas aeruginosa, mot+, Re = 5.5			
1	Down	5.6	1.1	0.21	0.14
	Control	2.4	0.6	0.20	0.16
	Up	3.2	1.0	0.23	0.22
2	Down	6.9	1.0	0.14	0.09
	Control	3.2	0.4	0.09	0.08
	Up	3.3	0.5	0.02	0.09
		Pseudomonas aeruginosa, mot+, Re = 16.6			
7	Down	10.1	4.3	1.25	0.92
	Control	5.7	2.0	1.03	0.68
	Up	8.9	3.0	1.35	0.74
		Pseudomonas fluorescens, mot+, Re = 5.5			
3	Down	1.6	0.3	0.22	0.09
	Control	1.8	0.3	0.41	0.09
	Up	2.0	0.5	0.48	0.18
4	Down	13.3	10.6	1.47	1.22
	Control	2.7	3.4	1.18	1.51
	Up	0.5[a]	0.1[a]	NC	NC
		Pseudomonas fluorescens, mot−, Re = 5.5			
5	Down	0.8[a]	0.1[a]	NC	NC
	Control	0.2[a]	0.02[a]	NC	NC
	Up	0.3[a]	0.1[a]	NC	NC
6	Down	0.1[a]	0.02[a]	NC	NC
	Control	0.3	0.2	0.10	0.19
	Up	0.1	0.1	0.04	0.12

[a] Data where no plateau was observed; B not calculable (NC).

between 1.5 and 2.8 times the J for Re = 5.5 (Table 1). Only half of the ratios were statistically significant; however, there was a consistent trend, and one can reasonably conclude that the initial coverage rate was greater for the higher velocity experiment. Interestingly, there was an inverse relationship between Reynold's number and plateau value; it was four times higher for Re = 5.5 than for Re = 16.6 (Table 2). Overall, an increase in the fluid velocity caused a corresponding increase in the initial coverage rate (*P. aeruginosa*), a decrease of the position effect, and a decrease in maximum coverage.

Pseudomonas fluorescens, mot+. Qualitative results from this organism were similar to those for *P. aeruginosa.* The density of cells in the bottoms of the grooves was about the same as that for the control position and there is a strong downstream position preference. Statistical analysis showed that there was considerable variability within and between the duplicate experiments. Because of that variability, the ratios of J values between positions were not statistically significant.

In general, the attachment rate for *P. aeruginosa* was greater than that for *P. fluorescens*, mot+, as shown by the median value of 1.6 for the ratio of the J values for these two organisms for all positions and experiments. However, the comparisons between the two motile bacteria were complicated by the fact that the J values for Experiment 4 were high for the downstream and control positions and were accompanied by high standard errors. At each position, the plateau values for *P. aeruginosa* were much higher than those for *P. fluorescens*, mot+ (Table 2).

Pseudomonas fluorescens, mot−. This organism was rarely found in the bottom of grooves, even after extended periods of colonization up to 21 h when cell division had likely occurred. The coverage rate for nonmotile cells was much smaller than for the parent motile strain, and a longer observation period was required to reach the same surface coverage. Even though observations were taken over extended times, the data analysis for Experiments 5 and 6 was conducted only for images collected in the first 12 h to minimize the influence of cell division.

In agreement with the other experiments, the results for *P. fluorescens*, mot− show that the largest J was at the downstream position. In the analysis of covariance, the position effect was statistically significant for the first replicate ($P < 0.001$), but not for the second ($P = 0.2$). Note that the plateau was not calculable for the downstream position based on the first 12 h of observation. However, the data indicate a

TABLE 2
Estimates of the Plateau (J/B), or Maximum Coverage Percentage, by Position; Duplicate Experiments Combined

Expt. No.	Postion	Plateau
	Pseudomonas aeruginosa, mot+, Re = 5.5	
1 and 2	Down	35.6
	Control	19.8
	Up	26.6
	Pseudomonas aeruginosa, mot+, Re = 16.6	
7	Down	8.1
	Control	5.5
	Up	6.6
	Pseudomonas fluorescens, mot+, Re = 5.5	
3 and 4	Down	8.8
	Control	2.9
	Up	2.7
	Pseudomonas fluorescens, mot−, Re = 5.5	
5 and 6	Down	NC[a]
	Control	2.0
	Up	5.8

[a] NC indicates not calculable; data did not show a plateau.

higher plateau for the upstream position than for the control (Table 2).

The observed J values for this nonmotile strain were smaller, often by one or two orders of magnitude, than those for the motile strain. The ratio of J values, mot+ to mot−, was statistically significant for about half of the comparisons ($P < 0.01$).

Sources of variability. The analysis of covariance showed that the total variability of $\log_{10}$ coverage was mainly attributable to the inherent, within-experiment variability and that there was relatively little variability between duplicate experiments. Define the total variance of $\log_{10}$ coverage as the sum of the variance within an experiment and the variance between duplicate experiments. For duplicate experiments with *P. aeruginosa* at Re = 5.5, only 33% of the total variance among $\log_{10}$ coverage was due to the difference between duplicate experiments. For the two runs with the motile *P. fluorescens* or with the nonmotile strain, the corresponding percentages are 1 and 10%, respectively. These percentages show that the $\log_{10}$ coverage values were similar between duplicate experiments and that the experimental method exhibited good repeatability.

Overall trends. In general, *P. aeruginosa* had a higher initial rate of attachment than *P. fluorescens,* mot+, which was greater than the rate for *P. fluorescens,* mot−. Only the motile organisms were found in the bottoms of the grooves. For all organisms, the initial rate of attachment was independent of the groove size. There was an important influence of position relative to the grooves; both the initial rate of attachment and the maximum coverage were greatest on the downstream edges of the grooves and least at the control sections for all bacterial strains.

Bead experiment. Since bacteria are often modeled as inert colloids, an experiment was conducted using fluorescent beads in place of bacteria at the same number of particles per milliliter of inoculum. After 4.5 h of exposure, only a few beads could be seen associated with the surface. For example, in one image at the same magnification as used for Fig. 5, only 14 beads at random locations were observed. No beads were detected in any of the grooves, nor was there any preferential attachment on the groove edges. The flow cell continued to run overnight and the coverage and position of the beads did not change appreciably. Again, no beads were found in the grooves. Since the number of beads associated with the surface even after nearly 24 h was so small, no J values or plateaus were calculated. There appeared to be no similarity between the behavior of any of the bacterial strains and the beads in terms of (i) initial coverage rate, (ii) plateau values, and (iii) preferential edge effects. The only possible similarity with the bacterial results is that neither the nonmotile strain or the inert colloids were found in the bottoms of the grooves.

Conditioning film study. Because the experiments were designed to investigate the importance of surface topographical features in the absence of chemical changes, it was important to verify that this condition persisted even after the surface had seen materials in the fluid that could preferentially adsorb to the groove edges. Surface analysis with ESCA showed that there was random contamination of the surface with poly(dimethylsiloxane) from the vacuum grease used to hold the coupon down in the flow cell. There was a small amount of organic nitrogen on the surface of the silicon coupon, suggesting that a very thin film of macromolecules was present on the surface as a conditioning film. Because the silicon substratum was also seen, the film was either very thin or discontinuous. Evidence of potassium and phosphorus from the buffer solution was also found. The distribution of this material on the surface was not specifically associated with the topographical features.

DISCUSSION

Appropriateness of the Adhesion Expression

The kinetics of cellular and particulate adhesion have been extensively studied (3, 20, 22, 31, 33) and can be generalized using a function of particle deposition (20). Expression [1] was used to calculate the initial colonization rate, designated J (32). A substantial amount of the comparative analyses in our studies depended upon the initial colonization rates provided by the deposition expression. With a few exceptions, the colloidal deposition expression provided an excellent fit to the data. The exceptional cases were better fit with a linear model. The plateau values obtained were less than 20% (except for *P. aeruginosa* at the downstream and upstream edges of the grooves, Re = 5.5), similar to the results found in the colloidal systems previously mentioned. In bacterial systems this plateau value was calculated in the absence or near absence of cell

growth, and this approach was used in our analysis. As growth dominates substratum coverage, the coverage vs time curve is expected to again rise sharply. This is exactly what happened in our long-term *P. fluorescens,* mot−, experiments. However, the results obtained after growth had commenced were not used in our analysis.

Strain Comparisons

It was very clear that the rates of attachment depended on the particular bacterial strain. *P. aeruginosa* attached at a higher rate than *P. fluorescens,* mot+, which attached faster than *P. fluorescens,* mot−, under otherwise identical conditions, including bacterial size.

The attachment rates of the two motile *Pseudomonas* species indicate that there are strain-dependent differences. Differences in attachment for these organisms has been substantiated by others. In flow cell studies the adsorption of *P. aeruginosa* was five times faster than that for *P. fluorescens* on glass, and approximately sixfold more rapid on 316 stainless steel, even though there was no difference in the measured motility velocity for the bacteria (23). Boelens *et al.* (2) found that *P. aeruginosa* attached 10 times faster than *P. fluorescens* in shaker flasks, but in this case bioluminescence was measured instead of cell numbers.

The importance of motility was even more dramatic. In otherwise identical *P. fluorescens* organisms, the presence of motility resulted in an order of magnitude increase in the initial rate of coverage. This agrees with the results of Korber *et al.* (17) where the same strains showed a two to three times enhanced attachment with motility. There are two common theories concerning the role of the flagella: (i) the ability to cross the energy barrier between the cell and the substratum to facilitate adhesion (22, 34) and (ii) an effective increase in the cell diffusivity through the boundary layer fluid (24, 28). It is possible that the lack of flagellar motion in the nonmotile strain (17) influenced the ability to cross the energy barrier, but it is more likely that the increased effective diffusivity of the motile strain resulted in more cell–surface collisions (23).

Effects of a Higher Velocity

Raising the velocity resulted in higher initial coverage rates for the same organism at the same cellular concentration in the bulk fluid. The increased rate is likely due to a higher mass loading, resulting in an increased frequency of organism collisions with the surface.

Effects of Topography on Attachment

The effect of topography was not at all expected. Discussions with industry have indicated that there is a general perception that rough surfaces colonize more rapidly than smooth surfaces due to more surface area available for attachment and that the greatest initial accumulation is in the bottoms of roughness elements because of protection from shear. This thought has also been proposed in the literature by Duddridge *et al.* (14). Schmidt (30) states that hydrodynamics in the vicinity of roughness elements fosters preferential attachment of yeast cells in valleys of stainless-steel surfaces when the roughness elements are greater than one. Work by Chabot and Bourget (8) showed that an increase in surface area had no effect on the attachment of cypris larvae, but no conclusive evidence exists for bacteria. The conventional picture always shows the bacteria in the bottoms of crevices (9); however, no direct observations have been made to determine whether this is a function of preferential initial attachment or the end result of ineffective cleaning. In our experiments, only the motile bacterial could be found regularly in bottoms of the grooves and even then in numbers comparable to those on the control surfaces. The nonmotile organisms and beads could not be found in the bottoms, suggesting that the presence of organisms in these features is a nonselective function of motility. This was somewhat surprising, as the hydrodynamic model suggested that there were eddies in the corners of the larger grooves that should have resulted in localized hydrodynamic entrainment of the cells and particles.

There was a significant effect of the presence of grooves on the rates of attachment of the cells, with preferential attachment on the downstream edges. The rates of attachment followed the general trend of being highest on the downstream edge and lowest at the control sections of the coupon. This effect was somewhat less pronounced for the higher shear experiment, but the trend was still present.

Even though there was a pronounced effect on attachment of the presence of grooves, there was no significant difference in attachment due to groove widths. This is somewhat puzzling since the modeling efforts showed that the predicted hydrodynamics were substantially different. The hydrodynamic model predicted essentially no disruption of the streamlines in the vicinity of a 10-μm-wide groove, with marked perturbation of flow, including corner eddies, for the 40-μm groove (Fig. 1). In all cases, there was a compression of the streamlines at the edges, indicating that there was increased flow velocity and pressure, but again the effect was more pronounced for the wider grooves. It may well be that a small trend between coverage and groove width really exists, but it was concealed by inherent statistical variability in the attachment process. Alternatively, it has been shown that there is an accumulation of charge on abrupt edges of surfaces (35), and this change in electrostatic potential could be similar for all edges, regardless of groove width. This concentration of charges could be responsible for the enhanced attachment to the edges. However, there was a significant difference in the rates of attachment for the three bacterial strains, and no attachment for the similarly charged/sized/hydrophobicity beads. If there is a role of charge accumulation, the influence is certainly not clear.

Potential Physiological Effects

The bead experiments yielded results substantially different from those of the bacteria, including the nonmotile strain. There was no edge effect noted with the beads and they were not found in the bottoms of the grooves. Although more bead experiments must be done before any strong conclusions can be drawn, it appears that inert particle behavior did not predict bacterial attachment. Every effort was made to match size, charge, and hydrophobicity of the beads with the cells, but it is possible that undetermined differences may be partially responsible for the lack of correlation. For example, it is likely that the surface characteristics of the cell are sufficiently complicated so that a simple measure of hydrophobicity is inadequate for predicting attachment behavior.

The existing theories regarding the attachment of cells to a substratum, DLVO and thermodynamics, assume that the transport of the cells to the substratum is not limiting. From the results of this work the transport in flowing systems, even at very low velocities, is indeed limiting. Care was taken to ensure that the surface chemistry was uniform and the cells within each experiment were at the same growth conditions. However, the cells showed preferential attachment to the downstream edges of the grooves where the boundary layer was thinner. Also, only the motile organisms adhered in the bottoms of the grooves whereas the nonmotile cells and beads did not. This difference cannot be explained as a physicochemical effect because there were no physicochemical differences between the tops and bottoms of the grooves.

SUMMARY

The flow cell experiments with the three organisms showed that there were differences in the attachment rates of the bacteria, but not the patterns. *P. aeruginosa* had a higher rate of attachment than *P. fluorescens*, mot+, which had a higher rate of attachment than *P. fluorescens*, mot−. The key finding was that the presence of grooves perpendicular to flow resulted in preferential attachment to the downstream edges of the grooves, and to a lesser extent to the upstream edges. For motile bacteria, the initial attachment rate at the control position between grooves on the surface was similar to the bottom of the grooves. Nonmotile bacteria were not found in the bottom of the grooves. When the cell concentration was held constant and the flow velocity increased, the rate of attachment increased, with a decrease in the importance of position relative to the grooves. The widths of the grooves displayed no effect, even though the hydrodynamic model predicted differences in flow relative to the widths. Inert beads did not behave like the nonmotile bacteria, except that both beads and nonmotile cells showed little coverage at the bottoms of the grooves. The beads did not preferentially attach at the edges of the grooves. The results suggest that the transport of the cells to the surface, especially transport due to motility, dominates physicochemical effects in predicting cell attachment in flowing systems.

ACKNOWLEDGMENTS

The help of the following people is greatly appreciated: Brian Schneider, who did most of the statistical analysis; Dr. Tim Minton, Department of Chemistry, who obtained the coupons; Dr. Gary Harkin, Department of Computer Science, who wrote the MARK software; Ernie Visser, who did the hydrodynamic modeling; Dr. Pat Schamberger, who performed all of the surface analysis; and Richard Buss at Sandia Laboratories in New Mexico, who etched the coupons. This project was funded through cooperative agreement ECD-8907039 with the National Science Foundation Engineering Research Centers program.

REFERENCES

1. Bar-Or, Y., *in* "Microbial Cell Surface Hydrophobicity" (R. J. Doyle and M. Rosenberg, Eds.), p. 211. American Society for Microbiology, Washington, DC, 1990.
2. Boelens, J., Zoutman, D., Campbell, J., Verstraete, W., and Paranchych, W., *Can. J. Microbiol.* **3,** 329 (1993).
3. Bowen, G. D., and Epstein, N., *J. Colloid Interface Sci.* **72,** 81 (1979).
4. Busscher, H. J., Sjollema, J., and van der Mei, H. C., *in* "Microbial Cell Surface Hydrophobicity" (R. J. Doyle and M. Rosenberg, Eds.), p. 335. American Society for Microbiology, Washington, DC, 1990.
5. Busscher, H. J., Weerkamp, A. H., van der Mei, H. C., Van Steenberghe, D., Quirynen, M., Pratt, I. H., Marechal, M., and Rouxhet, P. G., *Colloids Surf.* **42,** 345 (1989).
6. Camper, A. K., Hamilton, M. A., Johnson, K. R., Stoodley, P., Harkin, G. J., and Daly, D. S., *Ultrapure Water* **9,** 27 (1994).
7. Camper, A. K., Hayes, J. T., Sturman, P. J., Jones, W. L., and Cunningham, A. B., *Appl. Environ. Microbiol.* **59,** 3455 (1993).
8. Chabot, R., and Bourget, E., *Marine Biol.* **97,** 45 (1988).
9. Characklis, W. G., and Marshall, K. C., "Biofilms." Wiley, New York, 1990.
10. Chen, B., Cunningham, A. B., Ewing, R., Peralta, R., and Visser, E., *Numer. Methods Partial Differential Equations* **10,** 65 (1994).
11. Cowan, M. M., van der Mei, H. C., Rouxhet, P. G., and Busscher, H. J., *J. Gen. Microbiol.* **138,** 2707 (1992).
12. Cowan, M. M., van der Mei, H. C., Stokroos, I., and Busscher, H. J., *J. Dent. Res.* **71,** 1803 (1992).
13. Cunningham, A. B., Visser, E., Lewandowski, Z., and Abrahamson, M., *Water Sci. Technol.* **32,** 107 (1995).
14. Duddridge, J. E., Kent, C. A., and Laws, J. F., *Biotechnol. Bioeng.* **XXIV,** 153 (1982).
15. Eginton, P. J., Gibson, H., Holah, J., Handley, P. S., and Gilbert, P., *Colloids Surfaces B: Biointerfaces* **5,** 153 (1995).
16. Gillis, R. J., M.S. thesis. Department of Microbiology, Montana State University, Bozeman, MT, 1993.
17. Korber, D. R., Lawrence, J. R., Sutton, B., and Caldwell, D. E., *Microb. Ecol.* **18** (1989).
18. Lumsden, J. B., and Stocker, P. J., *Metallurgica* **15,** 1295 (1981).
19. "S-plus Guide to Statistical and Mathematical Analysis." MathSoft, Inc., Seattle, WA, 1995.
20. Meinders, J. M., Noordmans, J., and Busscher, H. J., *J. Colloid Interface Sci.* **152,** 265 (1992).
21. "Minitab Reference Manual." Minitab, Inc., State College, PA, 1995.
22. Mozes, N., and Rouxhet, P. G., *in* "Biofilms—Science and Technology" (T. R. Bott, L. Melo, M. Fletcher, and B. Capdeville, Eds.), p. 69. Kluwer, The Netherlands, 1992.
23. Mueller, R. F., *Water Res.* **30,** 2681 (1996).

24. Mueller, R. F., Characklis, W. G., Jones, W. L., and Sears, J. T., *Biotechnol. Bioeng.* **39,** 1161 (1992).
25. Mueller, R. F., M.S. thesis. Department of Environmental Engineering, Montana State University, Bozeman, MT, 1990.
26. Neter, J., Kutner, M., Nachtsheim, C., and Wasserman, W., "Applied Linear Statistical Models—Fourth Edition." Irwin, Homewood, IL, 1996.
27. Pedersen, K., *Water Res.* **24,** 239 (1990).
28. Piette, J.-P. G., and Idziak, E. S., *Appl. Environ. Microbiol.* **57,** 1635 (1991).
29. Scheuerman, T., M.S. thesis. Department of Chemical Engineering, Montana State University, Bozeman, MT, 1996.
30. Schmidt, R., *Acta Biotechnol.* **12,** 203 (1992).
31. Sjollema, J., and Busscher, H. J., *Colloids Surfaces* **47,** 323 (1990).
32. Sjollema, J., Busscher, H. J., and Weerkamp, A. H., *J. Microbiol. Methods* **9,** 79 (1989).
33. Sjollema, J., Busscher, H. J., and Weerkamp, A. H., *J. Microbiol. Methods* **9,** 73 (1989).
34. Sjollema, J., van der Mei, H. C., Uyen, H. M. W., and Busscher, H. J., *J. Adhesion Sci. Technol.* **4,** 765 (1990).
35. Smythe, W. R., *in* "Static and Dynamic Electricity," p. 82. McGraw–Hill, New York, 1950.
36. Sorongon, M. L., Bloodgood, R. A., and Burchard, R. P., *Appl. Environ. Microbiol.* **57,** 3193 (1991).
37. van der Mei, H. C., Cowan, M. M., Genet, M. J., Rouxhet, P. G., and Busscher, H. J., *Can. J. Microbiol.* **38,** 1033 (1992).
38. van der Mei, H. C., Meinders, J. M., and Busscher, H. J., *Microbiology* **140,** 3413 (1994).
39. Vanhaecke, E., Remon, J.-P., Moors, M., Raes, F., de Rudder, D., and van Reteghem, A., *Appl. Environ. Microbiol.* **56,** 788 (1990).
40. Walsh, D., Pope, D., Danford, M., and Huff, T., *JOM* **45,** 22 (1993).